

published).

<sup>13</sup>This number and its associated error are taken to span all modern experimental results with which the authors are familiar.

<sup>14</sup>Y. K. Kim and M. Inokuti, Phys. Rev. **165**, 39 (1968).

<sup>15</sup>A. J. Rabheru, M. M. Islam, and M. R. C. McDowell, to be published.

<sup>16</sup>A. L. Sinfailam and R. K. Nesbet, Phys. Rev. A **6**, 2118 (1972).

<sup>17</sup>F. J. de Heer and R. H. J. Jansen, Fundamenteel Onderzoek der Materie Report No. 37173, 1975 (unpublished).

<sup>18</sup>D. Andrick and A. Bitsch, J. Phys. B: At. Mol. Phys. **8**, 393 (1975).

<sup>19</sup>The derivation given in Refs. 3 and 4 takes this point of view in that it essentially obtains a dispersion relation for  $\bar{f}(E) = f(E) - [f_{B1}^d(E) - g_1(E)]$ , using properties of the full Green's function.

## Feshbach and Shape Resonances in the $e\text{-H } ^1P$ System

C. D. Lin

*Center for Astrophysics, Harvard College Observatory and Smithsonian Astrophysical Observatory,  
Cambridge, Massachusetts 02138*

(Received 9 June 1975)

Using a Born-Oppenheimer-type expansion for the two-electron wave functions in hyperspherical coordinates, three potential curves are obtained for  $\text{H}^-$   $^1P$  states converging to the  $n=2$  state of the hydrogen atom. It is shown that the Feshbach resonances are associated with one curve and the shape resonance with another. The connections with the "+" and "-" classification of helium doubly excited states and with the asymptotic dipole-field representation of  $\text{H}^-$  are discussed.

Various elaborate methods have been employed to obtain accurate positions and decay widths of resonances in electron-hydrogen-atom collisions.<sup>1</sup> The most careful and thorough study of this system is the close-coupling calculations by Burke and co-workers.<sup>2</sup> Besides the numerous Feshbach resonances below the  $n=2$  threshold of H, they predicted the existence of a narrow shape resonance of  $^1P$  symmetry, with energy only 18 meV above the  $n=2$  threshold. This shape resonance greatly influences the  $1s \rightarrow 2s$  and  $1s \rightarrow 2p$  excitation cross sections in electron-hydrogen scattering<sup>2</sup> and also the photodetachment cross section of  $\text{H}^-$  near the  $n=2$  threshold.<sup>3</sup>

As is well known, a shape resonance can be produced from potential scattering if the potential possesses a barrier at large distances  $R$  from the force center and is attractive enough at small  $R$ . In electron-hydrogen scattering, the existence of potential barriers at large  $R$  in certain channels has been known for many years.<sup>4</sup> Because of the complicated interactions at small  $R$ , however, it has not been possible to get an estimate of the strengths of the potential wells, if any, at small  $R$ , so as to connect the two regions. In this note, we will show that, by using hyperspherical coordinates, it is possible to approximate the electron-hydrogen scattering by one-di-

mensional (1D) potential scattering. In particular, for  $^1P$  states, three potential curves associated with the  $n=2$  state of H are obtained, one being completely repulsive at all  $R$ , one having the property that it can produce a shape resonance, and one having the ability to support an infinite number of Feshbach resonances.

In a recent paper<sup>5</sup> (to be called I), I have used hyperspherical coordinates to study the properties of doubly excited states of helium. In this coordinate system, the distances of the two electrons from the nucleus  $r_1$  and  $r_2$  are replaced by a hyperradius  $R = (r_1^2 + r_2^2)^{1/2}$  and a hyperangle  $\alpha = \arctan(r_2/r_1)$ . The angle  $\alpha$ , together with the usual polar coordinates  $(\theta_1, \varphi_1)$  and  $(\theta_2, \varphi_2)$  of the two electrons represented collectively as  $\Omega \equiv \{\alpha, \theta_1, \varphi_1, \theta_2, \varphi_2\}$ , identify the orientation of the electron pair on a 5D spherical surface, whereas the coordinate  $R$  measures the size of the system. An interchange of the positions of electrons 1 and 2 amounts to changing  $\alpha$  into  $\frac{1}{2}\pi - \alpha$  and interchanging  $(\theta_1, \varphi_1)$  and  $(\theta_2, \varphi_2)$ , with  $R$  fixed.

Using atomic units and expanding the two-electron wave function  $\psi(R, \Omega)$  as

$$\psi = R^{-5/2} \sum_{\mu} F_{\mu}(R) \Phi_{\mu}(R; \Omega), \quad (1)$$

where  $R$  is treated as a parameter in  $\Phi_{\mu}(R; \Omega)$ , we can reduce the Schrödinger equation for the

two-electron system to

$$[d^2/dR^2 - V_\mu(R) + W_{\mu,\mu'}(R) + 2E]F_\mu(R) + \sum_{\mu'} W_{\mu,\mu'}(R)F_{\mu'}(R) = 0. \quad (2)$$

Equation (2) has a structure similar to that of molecular-wave-function expansion for diatomic molecules, where  $V_\mu(R)$  is the potential curve and  $W_{\mu,\mu'}(R)$  is the coupling term between channels  $\mu$  and  $\mu'$ . If the coupling term  $W_{\mu,\mu'}$  can be neglected in the first approximation, as is indeed the case in the calculation of helium potential curves<sup>6</sup> and in the present calculation, Eq. (2) reduces to a family of ordinary differential equations similar to the single-particle radial Schrödinger equation with potential  $U_\mu(R) = V_\mu(R) - W_{\mu,\mu}(R)$ . The electron-hydrogen scattering is thereby reduced to potential scattering with potential  $U_\mu$  for each channel  $\mu$ , and the properties of bound states or scattering states for each channel  $\mu$  are related directly to the shape of the potential  $U_\mu(R)$  and the behavior of the channel function  $\Phi_\mu(R; \Omega)$ .

In contrast to the close-coupling formulation, the potential  $U_\mu(R)$  is local. The symmetry condition on the two-electron wave function  $\psi(R, \Omega)$  imposed by the Pauli exclusion principle is explicitly included in the channel function  $\Phi_\mu(R; \Omega)$  and the potential curve  $U_\mu(R)$ . In the actual calculation, for states with total orbital angular momentum  $L$  and total spin  $S$ , I expanded

$$\Phi_\mu(R; \Omega) = \sum_{[l_1 l_2]} [g_{l_1 l_2 \mu}(R; \alpha) \mathcal{Y}_{l_1 l_2 L M}(\hat{r}_1, \hat{r}_2) + (-1)^{l_1 + l_2 - L + S} g_{l_1 l_2 \mu}(R; \frac{1}{2}\pi - \alpha) \mathcal{Y}_{l_2 l_1 L M}(\hat{r}_1, \hat{r}_2)], \quad (3)$$

where  $l_1$  and  $l_2$  are the angular-momentum quantum numbers of the two electrons and  $\mathcal{Y}_{l_1 l_2 L M}(\hat{r}_1, \hat{r}_2)$  is the total orbital angular-momentum wave function. The summation over  $[l_1 l_2]$  in (3) is not ordered; i.e.,  $[l_1 l_2]$  is not distinguished from  $[l_2 l_1]$ . In the calculation for  $^1P$  states, the summation was truncated to include only  $[l_1 l_2] = [1, 0]$  and  $[2, 1]$ , consistent with the terms considered in the three-state close-coupling calculations. With this expansion, the amplitudes  $g_{l_1 l_2 \mu}(R; \alpha)$  at each  $R$  satisfy a system of coupled differential equations, in which the number of equations equals the number of terms retained in the expansion in (3). The eigenvalues  $V_\mu(R)$  and amplitudes  $g_{l_1 l_2 \mu}(R; \alpha)$  are solved most conveniently by finite-difference methods. At large  $R \approx r_1$  ( $R \rightarrow \infty$ ,  $\alpha \rightarrow 0$ ), it can be shown that these coupled equations in  $\alpha$  coincide with the coupled equations (to order  $1/R^2$  in the potential) in the close-coupling formulation. Thus, the potential  $U_\mu(R)$  and channel function  $\Phi_\mu(R; \Omega)$  coincide with those in the dipole representation of Gailitis and Damburg<sup>4b</sup> at large  $R$ . The results of their large- $R$  analysis are then applicable. However, in the present approach the potential and channel function are defined throughout the whole range of  $R$ . Thus, the use of hyperspherical coordinates provides a connection in the study of the properties of two-electron systems throughout the whole range of  $R$ .

The three potential curves  $U_\mu(R)$  (atomic units are used throughout unless otherwise given) converging to the  $n=2$  state of H are shown in Fig. 1 where the curves labeled "+" and "-" in the region  $12.5 < R < 14.5$  are obtained by interpolating diabatically. It is shown in I that the + series is

associated with an antinode near  $\alpha = 45^\circ$  and the - series is associated with a node near  $\alpha = 45^\circ$  in  $g_{10\mu}(R; \alpha)$  of Eq. (3). In order to maintain a smoothly varying channel function  $\Phi_\mu(R; \Omega)$  so as to avoid large coupling terms  $W_{\mu,\mu'}$  in Eq. (2), the + and - curves in Fig. 1 are found to cross at  $R = 13.5$ , thus preserving their + or - characters throughout the whole range of  $R$ . This crossing can also be understood in terms of a single-particle model, as is to be discussed later.

In Fig. 1, the curve denoted "-" has a shallow and broad minimum which behaves asymptotically as  $-3.71/R^2$  at large  $R$  below the  $n=2$  threshold. This potential can support an infinite number of Feshbach resonances, the first two of which are calculated to be  $-0.25191$  and  $-0.25006$  Ry, by solving the eigenvalues from the - curve.

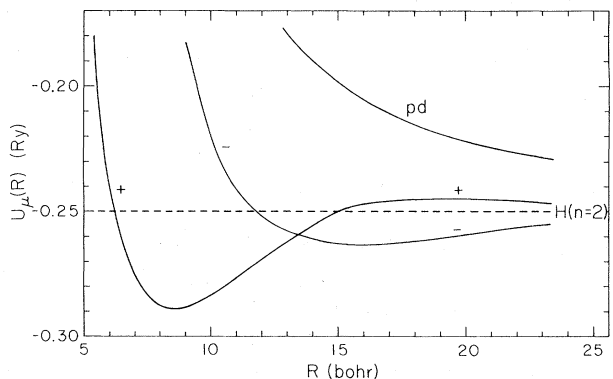


FIG. 1. Potentials for  $H^-$   $^1P$  channels converging to the  $n=2$  limit of H.

The values agree well with the variational results,  $-0.25193$  and  $-0.25003$  Ry, of O'Malley and Geltman,<sup>7</sup> indicating that for Feshbach resonances the neglect of the coupling term is a good first approximation. The curve denoted by "+" is more attractive at small  $R$  than the  $-$  curve, but it has a potential barrier with height  $4.8 \times 10^{-3}$  Ry and behaves asymptotically as  $2/R^2$  above the  $n=2$  threshold. The potential well is not attractive enough to support a bound state below the  $n=2$  threshold but may be strong enough to support a shape resonance above the  $n=2$  threshold. To see that this is indeed so, one can integrate the equation in  $R$  numerically with the  $+$  potential to find the phase shifts. These phase shifts are plotted versus energy above the  $n=2$  threshold in Fig. 2(a) where a fast variation of phase shifts with energy can be observed. These resonance features can also be identified in Fig. 2(b) where plots of  $F_\mu(R)$  show localized resonance behavior near  $R=12$  as resonance energy is approached. From the computed phase shifts, the resonance position  $E_r$  and width  $\Gamma$  are found to be 32 and 28 meV, respectively. These values are greater than the values  $E_r = 18$  meV and  $\Gamma = 15$  meV obtained by the three-state close-coupling calculation with twenty correlation terms, but are more accurate than the three-state close-coupling calculations without correlation.<sup>2</sup>

The third curve denoted by " $pd$ " is completely repulsive and behaves asymptotically as  $9.71/R^2$ . The channel function for this curve has a large component of  $[L_1, L_2] = [2, 1]$ , and may be denoted as " $pd$ ." This channel has the most repulsive potential among the three curves and will not contribute significantly to any excitation processes near the  $n=2$  threshold.

Since the excitation processes occur at small  $R$  ( $R \approx 4$ ), from Fig. 1 it is evident that the main contribution to the excitation cross sections comes from the  $+$  channel, with little from the other two. However, because of the presence of the potential barrier, the  $+$  channel is not open until the barrier can be penetrated. In this narrow energy region, only the  $-$  channel is open, i.e., the one which can support an infinite number of bound states. It has been shown that such a channel will have finite excitation cross sections ( $1s \rightarrow 2s$  and  $1s \rightarrow 2p$ ) at the threshold.<sup>4b</sup> In the  $^1P$  states studied here, however, this threshold law only has a very limited range of applicability because the  $+$  channel will dominate the ex-

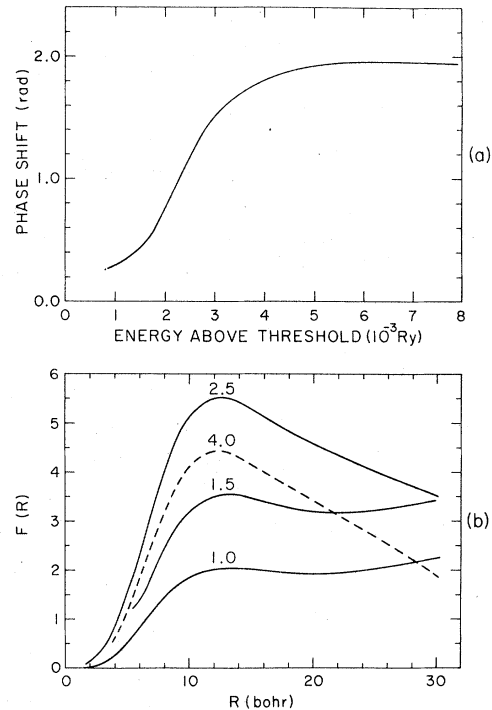


FIG. 2. (a) Computed phase shifts for the  $+$  channel. (b) Radial wave functions  $F(R)$  at various energies in units of  $10^{-3}$  Ry, showing the behavior of resonance. These continuum wave functions are normalized per unit energy, with energies expressed in atomic units.

citation processes within a few meV.

The crossing between the two curves in Fig. 1 can also be expected in terms of the independent particle model. I have denoted these two curves by " $+$ " and " $-$ ," implying a close resemblance to the  $+$  and  $-$  series classification introduced by Cooper, Fano, and Prats<sup>8</sup> in the interpretation of the photoionization data of helium doubly excited states.<sup>9</sup> They show that the observed broad series corresponds to the in-phase coherent oscillation of the radial motion of the two electrons which can be denoted simply as  $2snp + 2pns$  and the narrow series which can be denoted as  $2snp - 2pns$ . The crossing between the  $+$  and  $-$  curves results from the difference in the types of correlation effect implied in the combinations  $2snp \pm 2pns$  in the region of small  $R$  and of large  $R$ .

Let  $2snp \ ^1^3P$  denote a single Slater determinant as constructed from single-particle orbitals;

then

$$\begin{aligned}
 (2snp + 2pns)^1 3P &= [2s(r_1)np(r_2)Y_{0110} + (-1)^S 2s(r_2)np(r_1)Y_{1010}] \\
 &\quad + [2p(r_1)ns(r_2)Y_{1010} + (-1)^S 2p(r_2)ns(r_1)Y_{0110}] \\
 &= [2s(r_1)np(r_2) + (-1)^S 2p(r_2)ns(r_1)]Y_{0110} \\
 &\quad + [2p(r_1)ns(r_2) + (-1)^S 2s(r_2)np(r_1)]Y_{1010}, \quad (4)
 \end{aligned}$$

where  $S$  is 0 and 1 for singlet and triplet, respectively, and  $nl(r_1)$  denotes the radial wave functions. As emphasized above, the + or - series of Ref. 8 implies the sign within each of the square brackets of Eq. (4). Therefore,  $2snp + 2pns$  is a + series and  $2snp - 2pns$  is a - series for  $1P$  at small  $R$ . The potential curve associated with  $(2snp - 2pns)^1P$  lies higher than that associated with  $(2snp + 2pns)^1P$  as a result of the existence of an extra node near  $\alpha = 45^\circ$ . On the other hand, at large  $R$  (or large  $r_2$ ), the exchange effect is not important and the terms with the factor  $(-1)^S$  in Eq. (4) can be neglected. It can be shown that in the asymptotic region, the potential associated with  $2snp + 2pns$  lies higher than that associated with  $2snp - 2pns$ , independent of  $1P$  or  $3P$ . Thus, for  $1P$ , the + curve lies lower at small  $R$  but higher at large  $R$  as compared with the - curve, resulting in a crossing between the + and - curves. On the other hand, since  $(2snp + 2pns)^3P$  is a - series at small  $R$  [because of the factor  $(-1)^S$ ,  $S=1$ ], it lies above the  $(2snp - 2pns)^3P$  series (the + series) at all  $R$  and no curve crossing is expected between them, as evidenced by actual calculation.<sup>10</sup>

It is interesting to note that the lowest Feshbach resonance of  $1P$  symmetry in  $H^-$  cannot be designated as  $2s2p 1P$ , so that the lowest doubly excited states cannot always be constructed from the allowed lowest combinations of single-particle states. This also explains why the  $2s2p 1P$  state of  $H^-$  was not found in the accurate  $1/Z$  expansion calculation of Drake and Dalgarno<sup>11</sup>; in other isoelectric sequences of helium the  $2s2p 1P$  is the lowest Feshbach resonance, but in  $H^-$  this state becomes a shape resonance. The lowest Feshbach resonance in this case should be designated as  $(2s3p - 2p3s)^1P$ . Its radius is peaked at  $R \approx 30$ , in contrast to the shape resonance in Fig. 2(b) which is peaked near  $R \approx 12$ .

I would like to thank Professor A. Dalgarno, Professor U. Fano, and Dr. G. Victor for their critical comments on the manuscript.

<sup>1</sup>For a recent review, see R. J. Risley, A. K. Edwards, and R. Geballe, Phys. Rev. A **9**, 1115 (1974).

<sup>2</sup>A. J. Taylor and P. G. Burke, Proc. Phys. Soc., London **92**, 336 (1967); P. G. Burke, A. J. Taylor, and S. Ormonde, *ibid.* **92**, 345 (1967); J. Macek and P. G. Burke *ibid.* **92**, 351 (1967).

<sup>3</sup>See J. Macek, Proc. Phys. Soc., London **92**, 365 (1967). An initial attempt to observe this resonance by photodetachment of  $H^-$  was not successful (J. Cooper of Joint Institute for Laboratory Astrophysics, private communication).

<sup>4a</sup>M. J. Seaton and I. C. Percival, Proc. Camb. Philos. Soc. **53**, 654 (1957).

<sup>4b</sup>M. Gailitis and R. Damburg, Proc. Roy. Soc. **82**, 192 (1963).

<sup>5</sup>C. D. Lin, Phys. Rev. A **10**, 1986 (1974). For earlier work, see J. Macek, J. Phys. B: At. Mol. Phys. **1**, 831 (1968); U. Fano, in *Atomic Physics: Proceedings*, edited by B. Bederson, V. W. Cohen, and F. M. Pichanick (Plenum, New York, 1969), Vol. I, p. 209. The actual method of calculation used here is different from that employed by Macek and Fano; a complete discussion with comparisons will be reported elsewhere.

<sup>6</sup>Macek, Ref. 5.

<sup>7</sup>T. F. O'Malley and S. Geltman, Phys. Rev. **137**, A1344 (1965).

<sup>8</sup>J. W. Cooper, U. Fano, and F. Prats, Phys. Rev. Lett. **10**, 518 (1963).

<sup>9</sup>R. P. Madden and K. Codling, Phys. Rev. Lett. **10**, 516 (1963).

<sup>10</sup>For  $3P$  of  $H^-$ , calculations show that the curve labeled "-" is completely repulsive. The results are to be reported elsewhere. For  $3P$  of He, the computed curves do not have any crossing; see Macek, Ref. 5.

<sup>11</sup>G. W. F. Drake and A. Dalgarno, Proc. Roy. Soc., London, Ser. A **320**, 549 (1971). See also, D. R. Herriek and O. Singanoglu, Phys. Rev. A **11**, 97 (1975).